Supplementary Information: Photophysics of the Red-form Kaede Chromophore

Kiri Addison, Palas Roy[1], Giovanni Bressan, Karolina Skudaite, Josh Robb, Philip B. C. Page, Eleanor K. Ashworth, James N. Bull* and Stephen R. Meech*

School of Chemistry, University of East Anglia, Norwich, Norfolk, NR4 7TJ

[1]Present address: *School of Basic Sciences, Indian Institute of Technology Bhubaneswar, Odisha 752050, India*

1. Experimental and Computational Details

Steady-state UV/vis absorption spectroscopy: Steady-state absorption spectra were recorded using a PerkinElmer Lambda XLS spectrophotometer. A 1 cm path length quartz cuvette was used and absorbance was kept below 1.

Steady-state fluorescence: Steady-state Fluorescence spectra were recorded using Spectrofluorometer Edinburgh Instruments FS5. Temperature control was with an Oxford Instruments DN1704 cryostat.

Time-resolved fluorescence upconversion: The detailed description of the time-resolved fluorescence upconversion set up was reported elsewhere.[1] In brief, the femtosecond oscillator (Coherent Micra-10 mode locked Ti:Sapphire Laser) produced pulses centred at 800 nm with a time duration of around 20 fs, repetition rate of 76 MHz and a power of about 900 mW. The pulsed laser output was compressed using a fused silica-based prism compressor and then focused onto a 50 µm thick type I BBO crystal to produce up to 15 mW of 400 nm second harmonic excitation pump beam. A dichroic mirror was used to separate the pump (second harmonic) and fundamental (which was used as the Gate pulse) beams. The gate beam was then passed through a pair of chirped mirrors (Femtolasers GSM216) and an optical delay line (Physik Instrumente). The pump beam was passed through another pair of chirped mirrors (Femtolasers GSM012). The pump beam was focused at the sample cell (1 mm path length) to generate fluorescence which was then focused onto a BBO crystal using a 15 times magnification reflective microscope objective. Finally, the fluorescence and gate beams were mixed in a type I BBO crystal (100 µm) to generate the up-converted signal at wavelengths from 296 to 336 nm depending on the fluorescence wavelength measured. The signal was detected by a photomultiplier and monochromator combination and measured with a photon counter. The up-converted signal was isolated from the intense scattering of pump beam utilising one filter (GG455, Schott) after the objective and another filter (UG11, Schott) at the entrance slit of the monochromator. The instrument response for the experiment was determined to be around 50 fs by recording the upconversion of Raman scattering from heptane.

Femtosecond transient absorption measurements (TA): Details about transient absorption set up used here has been described elsewhere.[2] Briefly, TA is a two pulse technique where a femtosecond actinic pump pulse excites the molecules electronically and then a time delayed broadband white light continuum probe pulse captures the resultant changes in the electronic spectra. The fundamental beam from the Spectra Physics Mai Tai laser oscillator was amplified using a regenerative Ti:sapphire amplifier (Spectra Physics Spitfire ACE). This generated output pulses centered at 800 nm with repetition rate of 1 kHz, duration of 120 fs, and energy of 5 mJ per pulse which was used to drive a commercial optical parametric amplifiers (OPA, Light Conversion TOPAS Prime). This OPA generates the tuneable actinic pump pulse in order to excite the samples. The polarization was set at magic angle using a combination of half wave plate and a polarizer. Another part of the fundamental 800 nm beam was directly focused on to a 3 mm thick sapphire window to generate broadband white light continuum (400-800 nm). A 50/50 beam splitter was used before the sample stage to split the WLC beam into a Reference WLC and a Probe WLC. Intensity fluctuations in the probe spectrum were corrected using the Reference WLC and reference detection channel. The Probe WLC was spatially and temporally overlapped with the actinic pump pulse in a 1 mm thick sample cell with fused silica windows. The focal spot sizes of the probe and pump pulses were 50 µm and 250 µm respectively. The pump beam energy at the sample cell was attenuated to 0.15 mW. The probe beam after the sample stage was aligned on top of each other with the reference beam collinearly. Both the probe and reference beams were dispersed using a prism based home-built spectrograph and then detected using two separate synchronised 16 bit A/D CCD detectors (1024 pixels) from Entwicklungsbüro Stresing. A computer-controlled delay stage in the pump path was used to generate delay between pump and probe. The pump beam was allowed to pass through a mechanical chopper at 500Hz to allow the detection of pump-on/pump-off probe and reference spectra. The referenced difference spectrum for each pulse pair was calculated using:

$$\Delta A = - \, log(\frac{Probe\ (Pump\ on)\ X\ Refernce\ (Pump\ off)}{Reference\ (Pump\ on)\ X\ Probe\ (Pump\ off)})$$

The detector was calibrated using Mercury-Argon lamp (HG-1 Ocean Optics). The solvent Kerr response with pump and probe beams provide the instrument response function (IRF) of about 100 fs. The data presented were average over 5 cycles and each time trace was accumulated for 0.1 sec. All pump-probe measurements were done in 1 mm flow cell in order to avoid any photodamage.

Global Analysis: Global analysis of the TA dataset was performed using Glotaran 1.5.1 software.[3] This reports both the Decay and Evolution Associated Difference Spectra (DADS and EADS respectively) and relaxation time associated with each species. Here we used two states model for both rK1H and rK1$^-$. The quality of good fit has been verified by looking at the wavelength dependent kinetic fittings.

Femtosecond stimulated Raman measurements (FSRS): The same setup used for TA measurement was modified for the FSRS measurements as has been described elsewhere.[4] In brief, FSRS is a three-pulse technique with femtosecond actinic pump, femtosecond white–light probe and picosecond

Raman pump pulses. The actinic pump excites the ground state molecule in its electronically higher excited state. Then a broadband femtosecond probe pulse in the presence of a narrowband (10 cm^{-1}) picosecond Raman pulse stimulate the coherent Raman scattering process from the sample. The actinic pump pulses were generated from OPA as described in the TA section. The probe for FSRS was generated using 1250 nm pulse (output from a second OPA) which was focused on to a 3 mm thick sapphire window to generate broadband white light continuum probe (500-1400 nm). On the other hand, picosecond Raman pump was generated by sending part of the amplified fundamental beam (from Spectra Physics Spitfire ACE amplifier) through a commercial second harmonic bandwidth compressor (SHBC from Light Conversion) and then a picosecond configured OPA (TOPAS-PS from Light Conversion). The Actinic pump, Raman pump and probe pulse were focused (spot sizes 250, 150 and 50 µm respectively) and overlapped spatially and temporally inside a 1 mm sample cell. No reference Probe was used for the FSRS measurements. The transmitted probe beam was dispersed using a high spectral resolution (<10 cm^{-1}) grating spectrometer (SPEX 500M) and then detected using a single CCD (1024 pixel). Stimulated Raman signal from cyclohexane was used to overlap the Probe and Raman pump pulses as well as to calibrate the detector. Spectral resolution as determined from the line width of the cyclohexane 802 cm^{-1} peak is about 10 cm^{-1}. A computer-controlled delay stage was used to provide delay between actinic pump and probe pulses. Each spectrum was accumulated for 6 s using LabView controlled software. The actinic pump power used was 1.4 mW at 440 nm (for rK1H) and 1.1 mW at 535 nm (for rK1^{-}). The Raman pulse was tuned at 700 and 650 nm (4 mW) to be in resonance with the excited state absorption of rK1H and rK1^{-} respectively. Time resolution of the experiment was determined to be about 100 fs as obtained from the solvent response dictated by the convolution between actinic pump and probe pulses.

All the spectra were recorded at 1 kHz. The Raman pump and actinic pump pulses were passed through two synchronized mechanical choppers operating at 250 Hz and 500 Hz respectively. This resulted four different signals: i) Raw FSRS (Probe + Raman + Actinic); ii) Transient absorption (Probe + Actinic); iii) Ground state FSRS (Probe + Raman) and iv) Probe reference (Probe only). The unprocessed FSRS signal is obtained when all the three pulse (Actinic pump, Raman pump and probe) are present on the sample as we detect log ($I_{Raman+Actinic+Probe}/I_{Probe}$). Therefore, the unprocessed FSRS signal contains information on the excited state Raman along with the ground state Raman (log ($I_{Raman+Probe}/I_{Probe}$)), transient absorption (TA) (log ($I_{Actinic+Probe}/I_{Probe}$)) and nonlinear background. Thus the unprocessed FSRS data has been subtracted from its ground state Raman and TA contributions in order to extract the excited state information. The resultant difference spectra (say, raw excited state Raman signal) are baseline corrected to obtain the raw excited state Raman signal as shown in main Figure 7. This same procedure is followed for different pump-probe time delays.

Time-resolved measurements at T = 77 K Millimolar concentration solutions of rK1H and rK1$^-$ were prepared in ethanol (≥99%, Fisher Scientific). The solution was deprotonated with a trace of 1 M aqueous sodium hydroxide. Time-resolved fluorescence measurements (at T = 77 K) were recorded using an Edinburgh Instruments FS5 spectrofluorometer, using excitation pulses from an EPLED-365 (λ = 365±10 nm, IRF (FWHM) ≈ 850 ps) and an EPL-485 (λ = 485±8 nm, IRF (FWHM) ≈ 150 ps) module, for rK1H and rK1$^-$, respectively.

2. Additional Figures

Figure S1 Proton NMR spectrum of rK1H in D2O

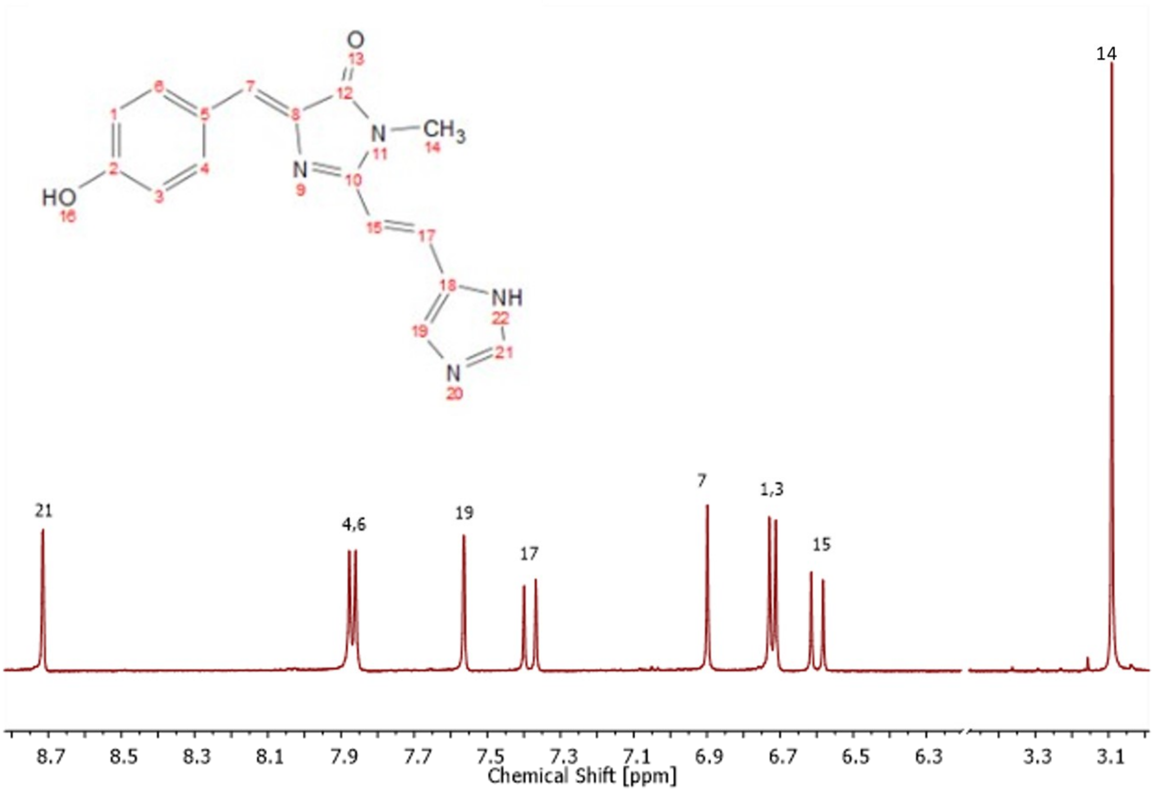

Figure S2 Intensity normalised emission spectra of rK1H (upper) and rK1⁻ showing the weak dependence of the emission wavelength on solvent polarity

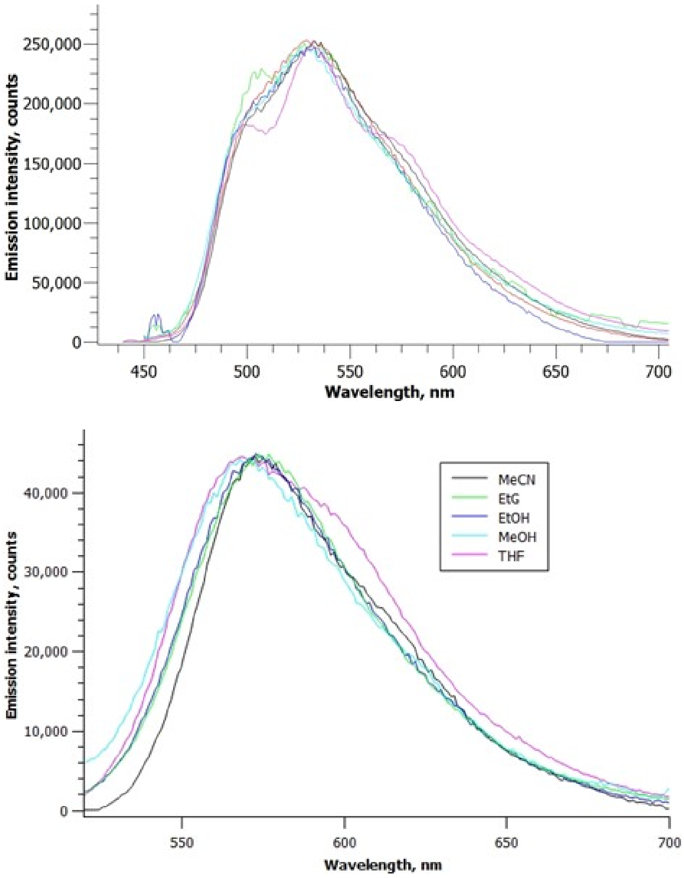

Figure S3 Time resolved emission spectra for kaede in methanol showing the development of the red shift with time as the blue emitting states decay more rapidly.

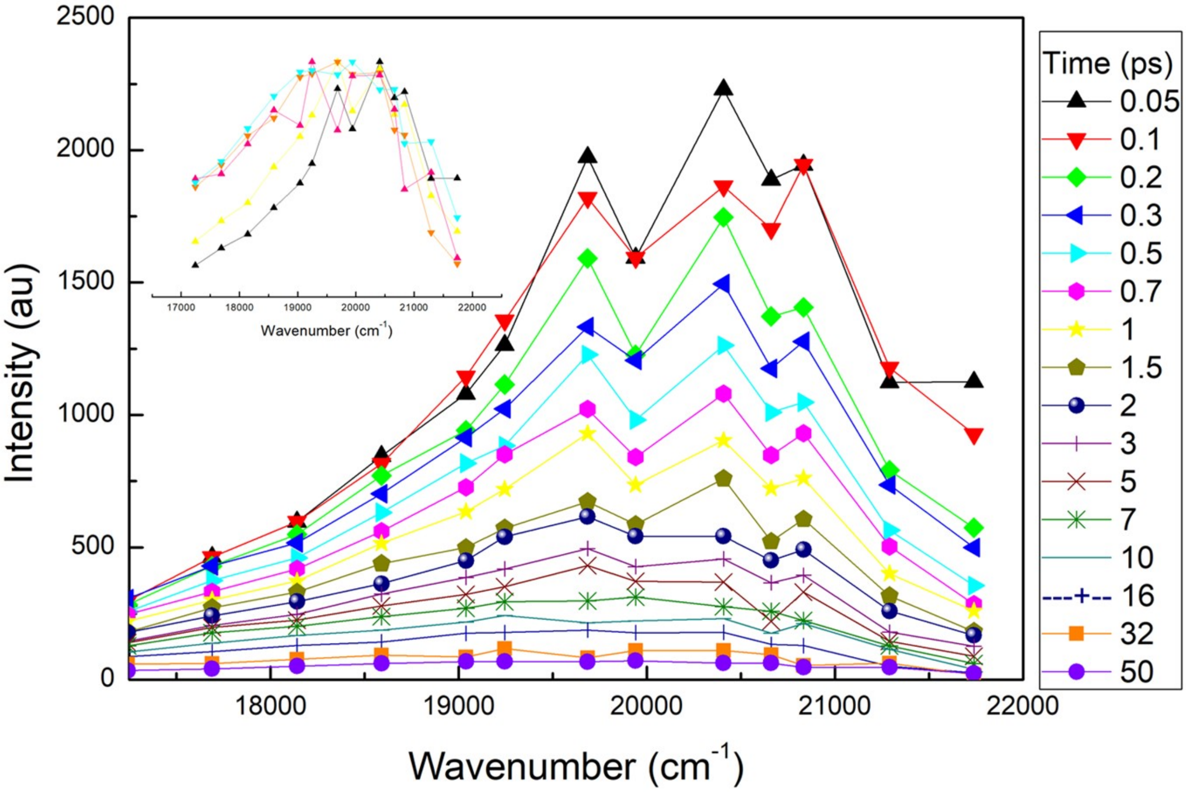

Figure S4 Concentration dependence of rK1H fluorescence decay plotted on log intensity and time scales. The absence of a concentration effect is clear.

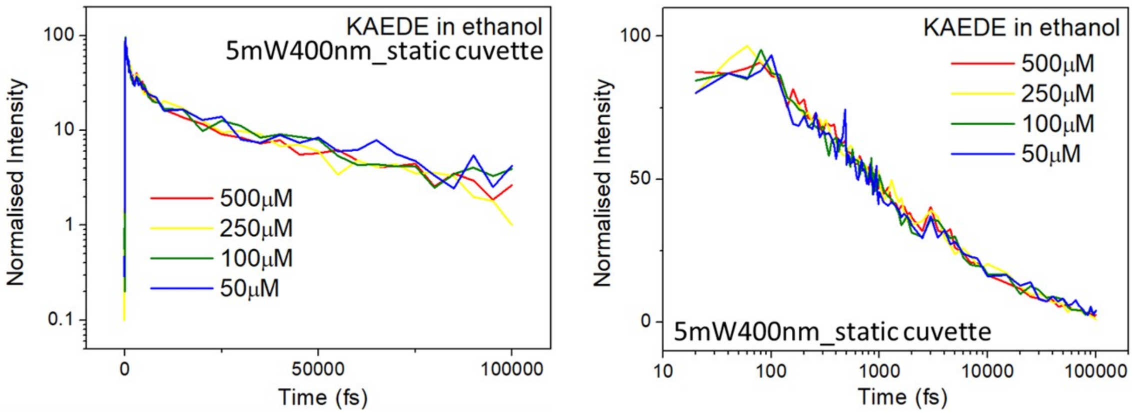

Figure S5 The dependence on flow rate and intensity for rK1H fluorescence decay, plotted on log intensity and time scales. The absence of a concentration effect is clear

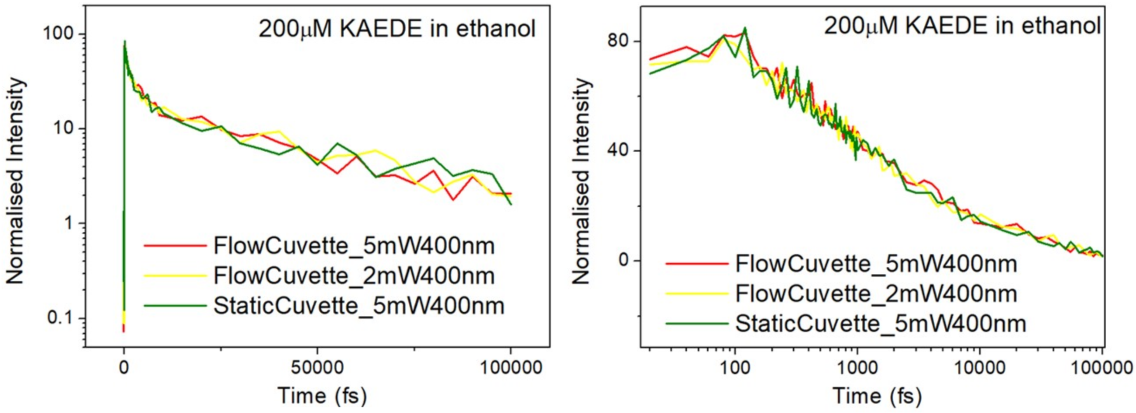

Figure S6 Transient absorption data showing the heatmap for rK1$^-$ and the time dependent data for both samples in ethanol. Global analysis of these data led to the DADS shown in Figure 6. The blanked out section is the scattered pump light.

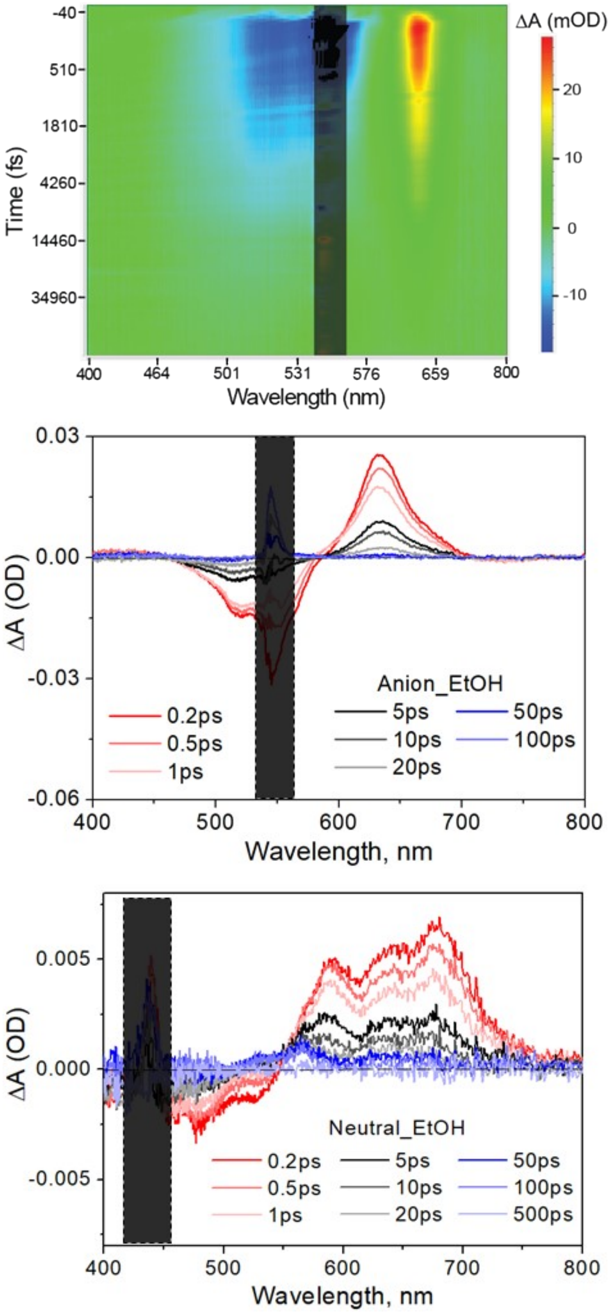

Figure S7 Arrhenius plots arising from the temperature dependent fluorescence yield measurements to recover the activation energy of the radiationless decay rate constant. (a) rK1H (b) $rK1^{-}$. F is the fluorescence quantum yield relative to the yield at 77 K. The *k* is the radiative rate constant (assumed 2.5×10^{9} s^{-1} to align with the observed ns decay at 77 K)

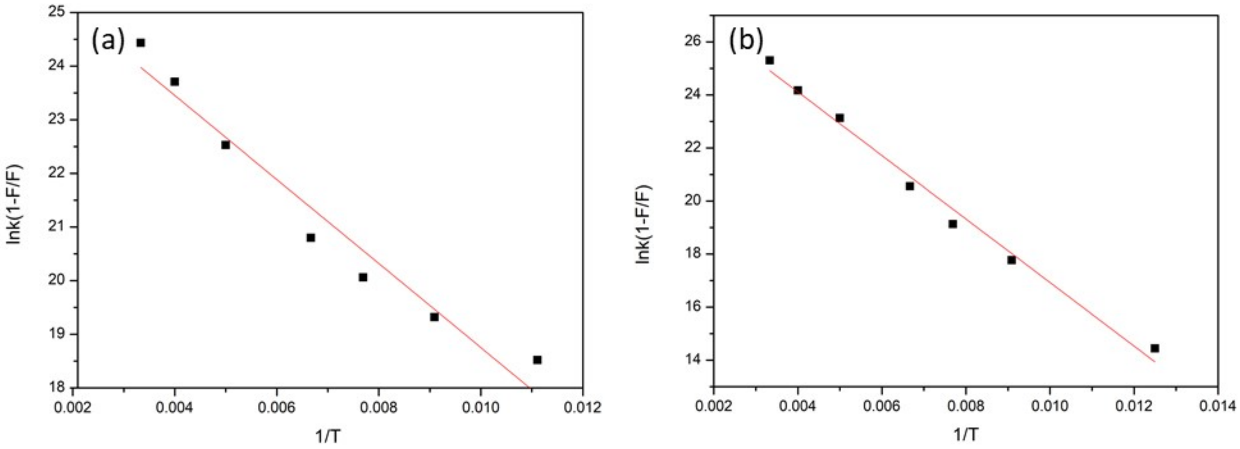

Figure S8 (a) Temperature dependence of the emission of rK1H in THF. (b) Arrhenius plot, which in this case was not well represented by a linear fit.

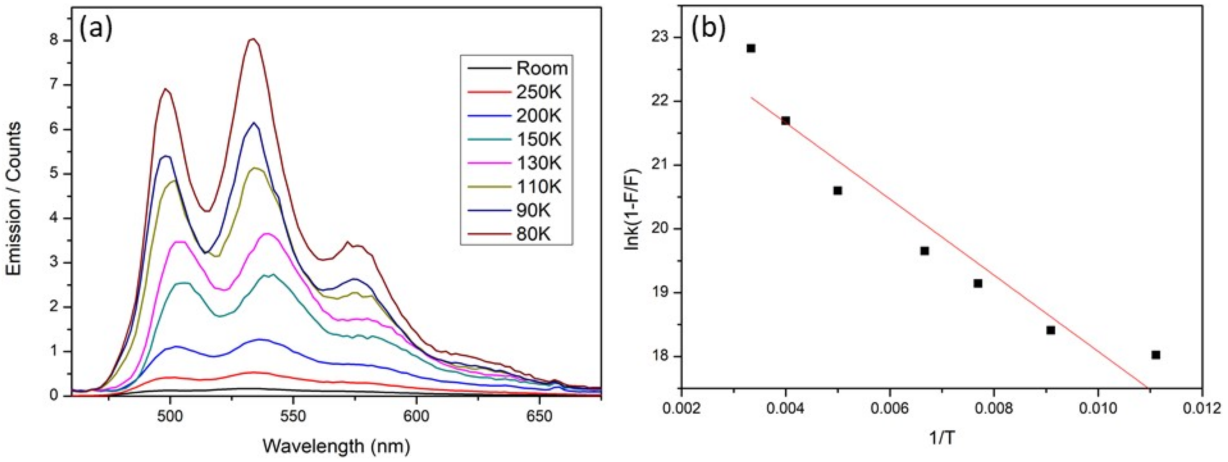

Figure S9 Temperature dependent excitation spectra (corrected for lamp intensity) for (a) rK1H and (b) rK1⁻ in ethanol

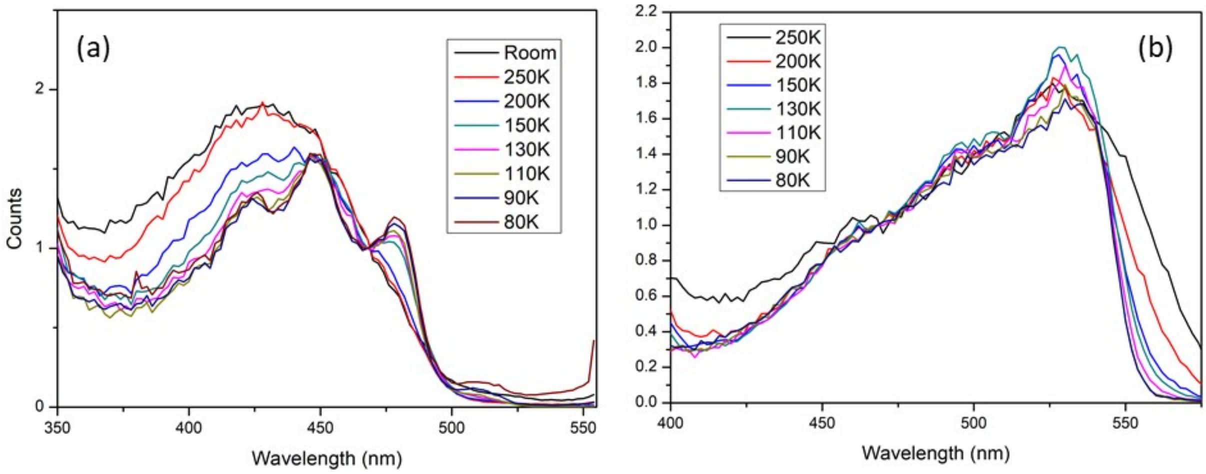

Figure S10 FCHT spectra at 300 K for (a) rK1H and (b) rK1⁻

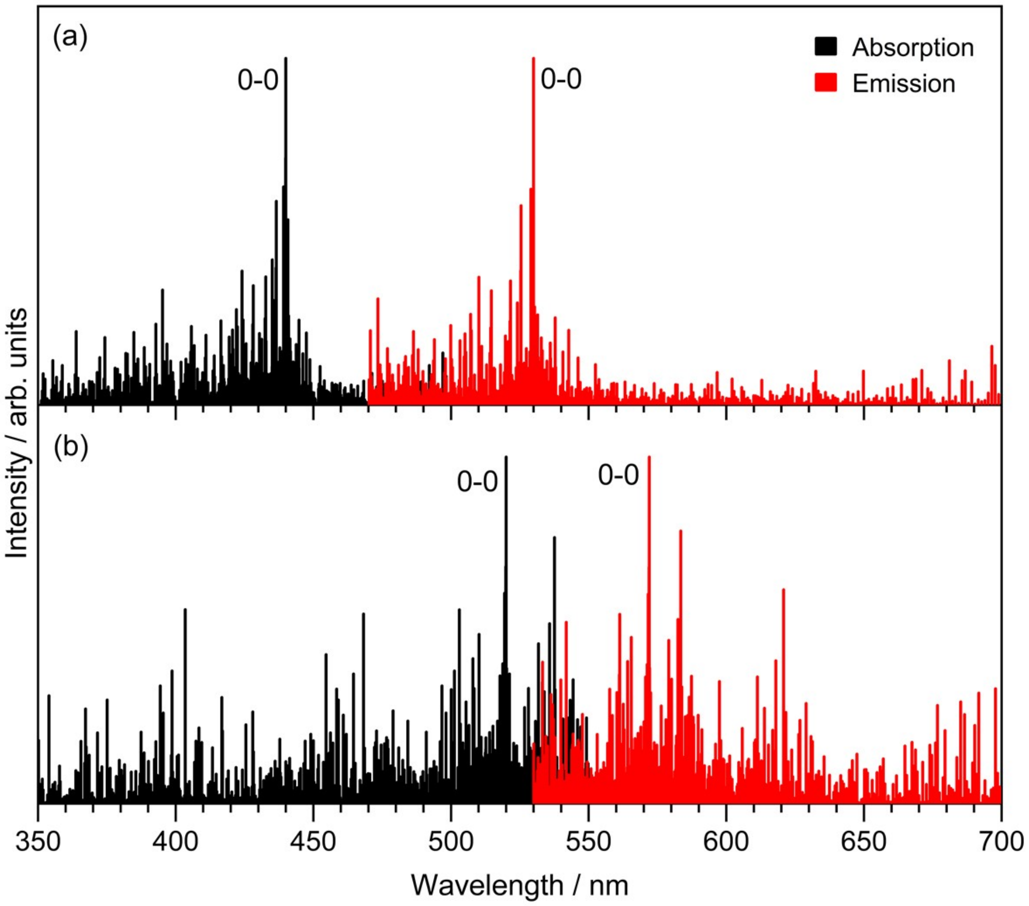

Figure S11 Nanosecond TRF measured at 77 K, showing the single exponential fit for (a) rK1H and (b) rK1⁻.

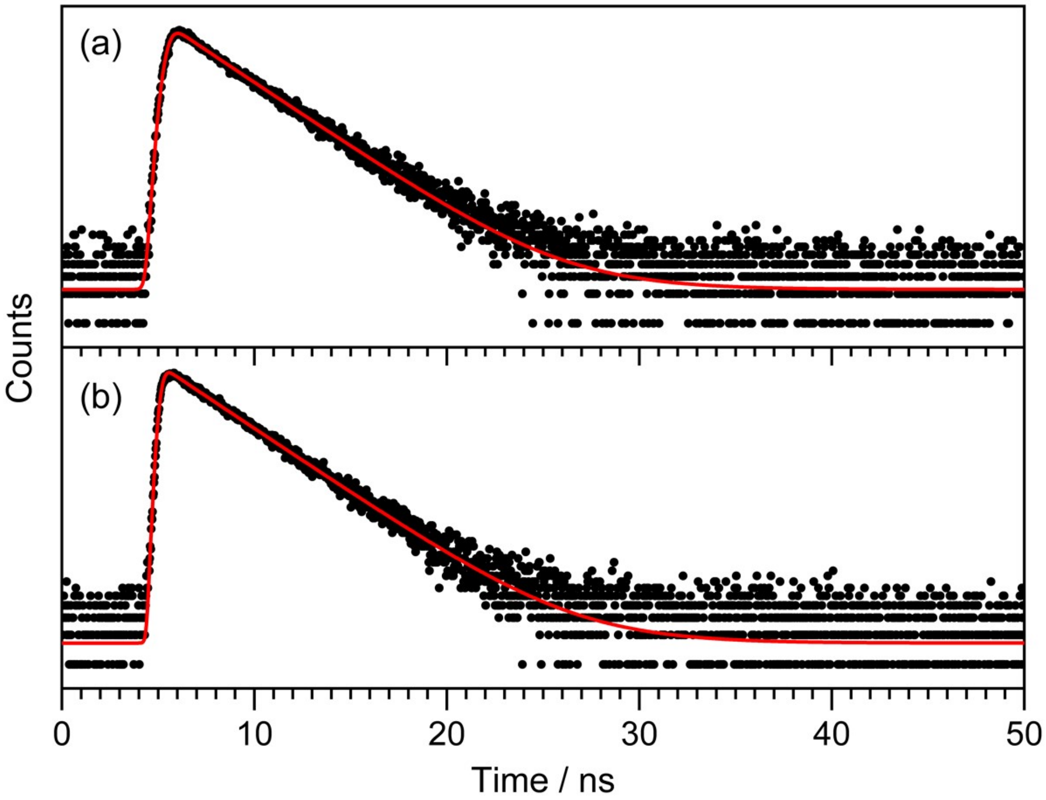

3. Additional tables

Table S1 Fitting parameters for the time resolved fluorescence of Kaede in various solvents measured at the peak emission wavelength. The error on the average lifetime is less than 11 %.

	MeOH	**H2O**	**EtOH**	**PrOH**	**BuOH**	**NMF**	**F**	**EG**
τ_1 (ps)	36	13.2	51.8	49.4	60.6	93.4	46.5	81.5
a_1	0.12	0.13	0.13	0.15	0.11	0.14	0.25	0.18
τ_2 (ps)	6.7	-	5.7	5.4	11.9	5.9	-	9.6
a_2	0.41	-	0.17	0.18	0.15	0.2	-	0.25
τ_3 (ps)	2.1	1.1	1.03	1.18	1.53	0.97	2.8	1.63
a_3	0.24	0.39	0.33	0.33	0.35	0.35	0.34	0.22
τ_4 (ps)	0.4	0.17	0.15	0.18	0.17	0.13	0.26	0.12
a_4	0.24	0.48	0.36	0.34	0.39	0.31	0.41	0.34
$\langle\tau\rangle$ (ps)	7.7	2.2	8.4	8.7	8.9	14.1	12.9	17.8

Table S2 Fitting parameters for the time resolved emission of Kaede in methanol measured from 470 nm to 580 nm. The average time constant has an error of less than 11 %.

	Emission Wavelength / nm							
	470	***480***	***500***	***520***	***525***	***540***	***550***	***580***
τ_1/ps	16	17	29	33	36	38	41	39
a_1	0.10	0.12	0.10	0.12	0.12	0.12	0.18	0.18
τ_2/ps	8.4	8.2	7.3	8.1	6.7	7	6.6	5.9
a_2	0.24	0.24	0.42	0.3	0.42	0.42	0.42	0.36
τ_3/ps	1.1	1.0	1.8	2.3	2.1	2.2	2.4	3.2
a_3	0.24	0.36	0.24	0.30	0.24	0.30	0.30	0.18
τ_4/ps	0.2	0.1	0.3	0.3	0.4	0.4	0.3	0.6
a_4	0.42	0.42	0.36	0.3	0.24	0.24	0.24	0.24
$\langle\tau\rangle$/ps	3.8	3.9	5.9	7.3	7.7	8.5	9.4	10.8

Table S3 Bi-exponential decay parameters extracted from global analysis of TA data (the corresponding fits are shown in figure 6d and the DADS in 6b,c

Sample	**DADS Components**
Neutral_EtOH	2ps, 57 ps
Neutral_GlyOH	2.9ps, 64ps
Anion_EtOH	1.3ps, 13ps
Anion_GlyOH	7.7ps, 142ps

4. References

1. I. A. Heisler, M. Kondo and S. R. Meech, Reactive Dynamics in Confined Liquids: Ultrafast Torsional Dynamics of Auramine O in Nanoconfined Water in Aerosol OT Reverse Micelles, *J. Phys. Chem. B*, 2009, **113**, 1623-1631.
2. P. Roy, G. Bressan, J. Gretton, A. N. Cammidge and S. R. Meech, Ultrafast Excimer Formation and Solvent Controlled Symmetry Breaking Charge Separation in the Excitonically Coupled Subphthalocyanine Dimer, *Angewandte Chemie-International Edition*, 2021, **60**, 10568-10572.
3. J. J. Snellenburg, S. P. Laptenok, R. Seger, K. M. Mullen and I. H. M. van Stokkum, Glotaran: A Java-Based Graphical User Interface for the R Package TIMP, *Journal of Statistical Software*, 2012, **49**, 1-22.
4. C. R. Hall, J. Conyard, I. A. Heisler, G. Jones, J. Frost, W. R. Browne, B. L. Feringa and S. R. Meech, Ultrafast Dynamics in Light-Driven Molecular Rotary Motors Probed by Femtosecond Stimulated Raman Spectroscopy, *J. Am. Chem. Soc.*, 2017, **139**, 7408-7414.